1-1-2015

Contribution of hepatic organic anion-transporting polypeptides to docetaxel uptake and clearance

Hannah H. Lee
Vanderbilt University School of Medicine

Brenda F. Leake
Vanderbilt University School of Medicine

Wendy Teft
Schulich School of Medicine & Dentistry

Rommel G. Tirona
Schulich School of Medicine & Dentistry, rommel.tirona@schulich.uwo.ca

Richard B. Kim
Schulich School of Medicine & Dentistry

See next page for additional authors

Molecular Cancer Therapeutics

Contribution of Hepatic Organic Anion-Transporting Polypeptides to Docetaxel Uptake and Clearance

Hannah H. Lee[1], Brenda F. Leake[1], Wendy Teft[2], Rommel G. Tirona[2], Richard B. Kim[2], and Richard H. Ho[1]

Abstract

The antimicrotubular agent docetaxel is a widely used chemotherapeutic drug for the treatment of multiple solid tumors and is predominantly dependent on hepatic disposition. In this study, we evaluated drug uptake transporters capable of transporting radiolabeled docetaxel. By screening an array of drug uptake transporters in HeLa cells using a recombinant vaccinia-based method, five organic anion–transporting polypeptides (OATP) capable of docetaxel uptake were identified: OATP1A2, OATP1B1, OATP1B3, OATP1C1, and Oatp1b2. Kinetic analysis of docetaxel transport revealed similar kinetic parameters among hepatic OATP1B/1b transporters. An assessment of polymorphisms (SNPs) in *SLCO1B1* and *SLCO1B3* revealed that a number of OATP1B1 and OATP1B3 variants were associated with impaired docetaxel transport. A Transwell-based vectorial transport assay using MDCKII stable cells showed that docetaxel was transported significantly into the apical compartment of double-transfected (MDCKII-OATP1B1/MDR1 and MDCKII-OATP1B3/MDR1) cells compared with single-transfected (MDCKII-OATP1B1 and MDCKII-OATP1B3) cells ($P < 0.05$) or control (MDCKII-Co) cells ($P < 0.001$). *In vivo* docetaxel transport studies in *Slco1b2*$^{-/-}$ mice showed approximately >5.5-fold higher plasma concentrations ($P < 0.01$) and approximately 3-fold decreased liver-to-plasma ratio ($P < 0.05$) of docetaxel compared with wild-type (WT) mice. The plasma clearance of docetaxel in *Slco1b2*$^{-/-}$ mice was 83% lower than WT mice ($P < 0.05$). In conclusion, this study demonstrates the important roles of OATP1B transporters to the hepatic disposition and clearance of docetaxel, and supporting roles of these transporters for docetaxel pharmacokinetics. *Mol Cancer Ther; 14(4); 994–1003. ©2015 AACR.*

Introduction

Docetaxel is a widely used chemotherapeutic drug for the treatment of multiple solid tumors, including breast, lung, head and neck, stomach, and prostate cancer. There is wide variability in the pharmacokinetics of docetaxel with up to 10-fold difference in drug clearance among patients receiving the same treatment regimens (1). Furthermore, studies have indicated that a mere 50% decrease in docetaxel clearance increased more than 4-fold the odds of developing grade 4 neutropenia (2). Accordingly, this substantial interindividual variability in docetaxel exposure may have important ramifications for clinical efficacy and drug-mediated toxicity.

Recent studies suggest that drug disposition genes play a major role in the variability of docetaxel disposition (3–5). Furthermore, genetic variation, or polymorphisms, in drug disposition genes contributes to interindividual variability in chemotherapy response and toxicity (6–8). As the disposition of docetaxel is closely related to differences between an individual's ability to metabolize and eliminate this drug (3, 4, 6–8), a major cause of pharmacokinetic variability may be an attribute to differential expression of polymorphic drug-metabolizing enzymes and/or drug-eliminating transporters, but it has still been unclear. Docetaxel is mainly metabolized by the hepatic phase I drug-metabolizing enzyme CYP3A4 and, to a lesser extent, by CYP3A5 (9) and eliminated by multidrug resistance protein 1 (MDR1, ABCB1, and P-glycoprotein; ref. 10). MDR1 is a membrane-localized and ATP-dependent drug efflux transporter with broad substrate specificity and primarily expressed in normal tissues such as the gastrointestinal tract, the liver, the kidney, and the brain (11, 12). Expression of MDR1 in such tissues results in reduced drug absorption (gastrointestinal tract), enhanced elimination into the bile (liver) and urine (kidney), and reduced accumulation of toxic agents (the brain; ref. 11).

Docetaxel is predominantly dependent on hepatic disposition in humans; approximately 75% docetaxel is excreted in bile, but only approximately 5% in urine (13). Until recently, little was known regarding the hepatic uptake of docetaxel. Organic anion–transporting polypeptides (OATP) are primarily expressed in organs of importance to drug disposition such as the liver, intestine, kidney, and brain, and mediate the sodium-independent transport of a diverse range of amphipathic organic compounds, including bile salts, steroid conjugates, thyroid hormones, anionic peptides, and numerous drugs (14, 15). Whereas OATP1A2, which is mainly expressed in brain, kidney,

[1]Division of Hematology and Oncology, Department of Pediatrics, Vanderbilt University School of Medicine, Nashville, Tennessee. [2]Division of Clinical Pharmacology, Schulich School of Medicine and Dentistry, Western University/University of Western Ontario, London, Ontario, Canada.

Note: Supplementary data for this article are available at Molecular Cancer Therapeutics Online (http://mct.aacrjournals.org/).

Corresponding Author: Richard Ho, Vanderbilt University Medical Center, 2220 Pierce Avenue, 338 PRB, Nashville, TN 37232-6310. Phone: 615-936-2802; Fax: 615-936-1767; E-mail: richard.ho@vanderbilt.edu

doi: 10.1158/1535-7163.MCT-14-0547

and small intestine, is expressed in cholangiocytes of liver, but not in hepatocytes (16), OATP1B1 and OATP1B3 are expressed highly in the hepatocytes of the liver and their localization is restricted to the basolateral membrane of hepatocytes (17). Accordingly, these transporters facilitate the hepatocellular accumulation of compounds such as drugs before metabolism and biliary secretion, and thus may largely contribute to drug disposition. As hepatic uptake appears to be an important factor in docetaxel clearance, it would be of interest to evaluate hepatic uptake transporters as determinants of docetaxel disposition. Indeed, previous studies indicated that OATP1B3 is capable of transporting docetaxel *in vitro* (3, 18). Recently, a study also reported that differential expression of the OATP1B family in the human liver regulates the initial step in the elimination of docetaxel, before metabolism (5).

In this study, we identified multiple OATPs capable of transporting docetaxel by screening an array of drug uptake transporters in HeLa cells using a recombinant vaccinia-based method. Among them, we aimed to gain more insight into the importance of hepatic OATPs to the disposition of docetaxel. Thus, we studied the roles of OATP1B transporters in the hepatic uptake, clearance, and plasma exposure of docetaxel *in vivo* and *in vitro*.

Materials and Methods

Chemicals and reagents

Radiolabeled [^{3}H]docetaxel (5 Ci/mmol, 15 Ci/mmol; >98% purity) was obtained from Moravek Biochemicals and Radiochemicals. Unlabeled docetaxel (>97% purity) was obtained from Sigma-Aldrich. All other chemicals and reagents, unless stated otherwise, were obtained from Sigma-Aldrich research and were of the highest grade available.

Cell culture and virus preparation

HeLa cells were purchased from the ATCC (July 2012) and cultured in DMEM supplemented with 10% FBS, penicillin (100 U/mL), and streptomycin (100 μg/mL; Invitrogen). The polarized MDCKII (Madin–Darby Canine Kidney II) cells were purchased from the Sigma-Aldrich (January 2013), and we generated several stable cell lines immediately after obtaining the cells. The original bank of MDCKII cells is from Public Health England (PHE; London, UK) and PHE authenticates their cell line, including testing for *Mycoplasma* by culture isolation, Hoechst DNA staining and PCR, culture testing for contaminant bacteria, yeast and fungi, species verification by DNA barcoding, and identity verification by DNA profiling. In addition, stable cell lines generated with the MDCKII cells for this study were confirmed by protein expression and transport activities using known specific substrates ([^{3}H]estrone-3-sulfate for OATP1B1; [^{3}H]cholecystokinin for OATP1B3). All MDCKII cells were cultured in DMEM containing high glucose and L-glutamine supplemented with 10% heat-inactivated FBS, penicillin (100 U/mL), and streptomycin (100 μg/mL; Invitrogen) and all cells, including HeLa cells, were maintained in a 5% CO_2 atmosphere at 37°C in a humidified incubator. Preparation of viral stock of vtf-7 virus was prepared as described previously (19). Briefly, HeLa cells grown to near confluence in 25-cm tissue culture plates were infected with 1 plaque-forming unit (PFU)/10 cells. After an incubation period of 48 h at 37°C, the infected cells were pelleted, homogenized, and recovered through centrifugation, followed by tittering of viral stock as described by Blakely and colleagues (20).

Wild-type and variant transporter plasmid construction

Preparation of expression plasmids containing human and rat uptake transporters, including pEF6/V5-His/OATP1B1 and pEF6/V5-His/OATP1B3, has been described previously (21). Briefly, the full open reading frames (ORF) of human and rat transporter cDNAs were obtained by PCR, using AmpliTaq DNA polymerase (PerkinElmer), from cDNA libraries synthesized from a variety of human and rat tissue mRNA, respectively. A pEF6/V5-His/MDR1 expression plasmid was also obtained by the same method as above. Generation of OATP1B1 and OATP1B3 variant expression plasmids used for *in vitro* functional studies has been described previously (21, 22). For consistency of expression, all transporters were packaged into the pEF6/V5-His-TOPO vector (Invitrogen). The expression plasmids for wild-type (WT) pcDNA3.1(+)/OATP1B1 and pcDNA3.1(+)/OATP1B3 were constructed by excising out the ORFs of the OATP1B1 and OATP1B3 cDNA sequences, respectively, from the plasmids pEF6/V5-His/OATP1B1 and pEF6/V5-His/OATP1B3 with Nhe1 and Xho1, and subcloning into pcDNA3.1(+) vector (Invitrogen). To generate an expression plasmid for pcDNA3.1-zeo(+)/MDR1 (WT), PCR was first performed with corresponding nucleotides containing start codon and internal EcoR1 site of MDR1 cDNA sequences using plasmid pEF6/V5-His/MDR1 as a template, and PCR products (1-1182nts) were then subcloned into pcDNA3.1-zeo(+) vector (Invitrogen). Second, DNA fragments (1171-3843nts) were obtained by digesting MDR1 cDNA with EcoR1 and Not1 from plasmid pEF6/V5-His/MDR1. Finally, pcDNA3.1-zeo(+)/MDR1 (WT) plasmid containing the full ORFs (1-3843nts) of MDR1 was generated by inserting the second DNA fragments (1171-3843nts) into the first pcDNA3.1-zeo(+)/MDR1(1-1182nts) plasmid digested with the same enzymes described above. All plasmids, including WTs and variants, were verified by sequencing in the DNA Sequencing Facility (VANTAGE) at Vanderbilt University Medical Center.

Measurement of docetaxel transport kinetics

Docetaxel transport kinetics were assessed in HeLa cells recombinantly expressing OATP1B/1b transporters. To measure transport kinetics, [^{3}H]docetaxel uptake during the linear phase (first 3 minutes) was assessed in the presence of various concentrations of unlabeled compound. Transporter-dependent uptake was determined in parallel experiments as the difference in drug uptake between transporter and parental plasmid DNA-transfected HeLa cells. Michaelis–Menten-type nonlinear curve fitting was used to estimate the maximal uptake rate (V_{max}) and concentration at which half the maximal uptake occurs (K_m) for OATP1B3 and Oatp1b2. For OATP1B1 uptake kinetics, weighted, nonlinear curve fitting was performed using a two-component model comprising of a saturable process and a nonsaturable process. All experiments were carried out in duplicate on at least 2 to 3 experimental days.

Generation of stably transfected MDCKII cells

MDCKII cell lines expressing hepatic uptake transporters or/and an efflux transporter as well as control cell (MDCKII-Co, MDCKII-MDR1, MDCKII-OATP1B1, MDCKII-OATP1B3, MDCKII-OATP1B1/MDR1, and MDCKII-OATP1B3/MDR1) were generated as follows: To generate the single-transfected cells, MDCKII-OATP1B1 and MDCKII-OATP1B3 cells, MDCKII cells were transfected with the plasmids pcDNA3.1(+)/OATP1B1 or

pcDNA3.1(+)/OATP1B3 using Lipofectamine 2000 reagent (Invitrogen) according to the manufacturer's instructions. At 18 to 32 hours after transfection, the cells were split and divided into 10-cm culture dishes with fresh media containing G-418 sulfate (800 μg/mL; Mediatech). After additional selection with G-418 sulfate, single colonies of transfectants were screened for OATP1B1 and OATP1B3 protein expression by immunoblot analysis to detect cell clones with the desired protein expression. Cell clones with highest protein expression comparable with the expression of the control cell lines were chosen for further experiments. For generation of double-(MDCKII-OATP1B1/MDR1 and MDCKII-OATP1B3/MDR1) transfected cell lines, single-(MDCKII-OATP1B1 and MDCKII-OATP1B3) transfected cells were retransfected with the plasmid pcDNA3.1-zeo(+)/MDR1 using the same transfection reagent mentioned above. For generation of MDCKII-MDR1 cells, MDCKII cells were also transfected with the plasmid pcDNA3.1-zeo(+)/MDR1. After additional selection with zeocin (800 μg/mL; Invitrogen), single colonies of all transfectants were screened for MDR1 expression as well as OATP1B1 and OATP1B3 by immunoblot analysis to detect cell clones with the highest expression. All expression values were normalized to the protein β-actin. Consequently, cell clones with the highest uptake transporters and/or an efflux transporter expression were chosen and used for drug transport studies. Control cells (MDCKII-Co) lacking any insert were obtained by first transfecting the MDCKII cells with pcDNA3.1(+) vector only, followed by retransfecting with pcDNA3.1-zeo (+)vector only.

Preparation of crude cell membrane fractions and cell surface proteins

Protein expression from MDCKII stable cells was assessed by immunoblot analysis of plasma membrane enriched preparations and biotinylated cell surface proteins. Crude cell membrane fractions were conducted as described previously with minor modification (23). Briefly, cells were scraped and collected in hypotonic lysis buffer (5 mmol/L Hepes, pH 7.2, 300 mmol/L mannitol, and 1x protease inhibitor cocktail; Roche) and homogenized with a pellet pestle (Thermo Fisher Scientific) and a syringe with 26G needle. The lysates were centrifuged at 800 × *g* for 10 minutes to remove cell debris, and the supernatant was saved. The supernatant was then centrifuged at 30,000 × *g* at 4°C for 30 minutes to obtain membrane pellets. The membrane pellets were dissolved in the same buffer without mannitol and protein concentration in pellets was determined using the Bicinchoninic Acid Assay (BCA) Protein Assay Kit (Thermo Fisher Scientific). Each 10 μg of extracted membrane proteins was used for immunoblot analysis.

For the isolation of cell surface fractions, cell surface biotinylation was performed as described previously (21). Briefly, an equal number of each MDCKII stable cell was plated into 6-well culture plates. Twenty-four hours later, each well was washed in ice-cold PBS-Ca^{2+}/Mg^{2+} (138 mmol/L $NaCl_2$, 2.7 mmol/L KCl, 1.5 mmol/L KH_2PO_4, 1 mmol/L $MgCl_2$, 0.1 mmol/L $CaCl_2$, pH 7.4) and treated with sulfo-N-hydroxysuccinimide-SS-biotin (Thermo Fisher Scientific) for 1 hour at 4°C. The cells were washed with ice-cold PBS-Ca^{2+}/Mg^{2+} containing 100 mmol/L glycine and lysed with RIPA buffer (10 mmol/L Tris base, 150 mmol/L NaCl, 1 mmol/L EDTA, 0.1% SDS, 1% Triton X-100, pH 8.0) containing 1x protease inhibitor cocktail (Roche). Following centrifugation, 140 μL of streptavidin–agarose beads (Thermo Fisher Scientific) were added to 600 μL of cell lysate and incubated for 1 hour at room temperature. Beads were washed four times with ice-cold lysis buffer, and biotinylated proteins were released from the beads by adding Laemmli sample buffer (Bio-Rad). Consequently, eluted biotinylated (cell surface expressed) proteins were subjected to immunoblot analysis for detection of OATP1B1, OATP1B3, or MDR1 by specific antibodies.

Immunoblot analysis

To confirm protein expressions from each stable cell line generated, immunoblot analysis was performed as described previously (14). Briefly, crude cell membrane proteins (each 10 μg) and biotinylated fractions were loaded on 10% SDS polyacrylamide gels and transferred to nitrocellulose membranes (PerkinElmer). After preincubation in PBS containing 0.05% Tween 20 and 5% nonfat dry milk, the blots were first incubated with the polyclonal rabbit anti-OATP1B3 antibody (1:2,500 dilution) and reprobed with different antibodies later, such as the polyclonal rabbit anti-OATP1B1 antibody (1:2,500 dilution) and the monoclonal anti-MDR1 antibody (1:1,000 dilution; Santa Cruz Biotechnology) at room temperature for 2 hours. The blots were washed with PBS containing 0.05% Tween 20 for 15 minutes (3 × 5 minutes) and then incubated for 1 hours with the secondary antibody an anti-Rabbit IgG for OATP1B1 and OATP1B3 and an anti-mouse IgG antibody for MDR1 conjugated with horseradish peroxidase (HRP; 1:10,000 dilution; Promega). The protein bands were detected using the Western lightning plus-enhanced chemiluminescence ECL (PerkinElmer). As a loading control, the blots were stripped and reprobed with the monoclonal mouse anti–Na^+/K^+-ATPase α antibody (1:5,000 dilution; Santa Cruz Biotechnology), followed by incubation with an anti-mouse IgG antibody conjugated with HRP (1:10,000 dilution; Promega).

Transport assays

Recombinant vaccinia-based uptake transport assay. Transport assays using a recombinant vaccinia virus were conducted as described previously (19). Briefly, HeLa cells grown in 12-well plates (0.8×10^6 cells/well) were infected with vaccinia (vtf-7) at a multiplicity of infection of 10 PFU/cell in Opti-MEM I medium (Invitrogen) and allowed to adsorb for 30 minutes at 37°C. Cells in each well were then transfected with 1 μg transporter cDNA packaged in pEF6/V5-His-TOPO vector (Invitrogen), along with Lipofectin (Invitrogen) and incubated at 37°C for 16 hours. The parental plasmid lacking any insert was used as control. Uptake (radioactivity) of docetaxel was measured after an incubation of 10 minutes. Total radioactivity was determined after the addition of cell lysates to vials containing 5 mL of Biodegradable Scintillation Cocktail (Amersham Biosciences). Retained cellular radioactivity was quantified by liquid scintillation counter (PerkinElmer). Transport activities were expressed in the percentage compared with the vector control. All experiments were carried out in duplicate on at least 2 to 3 experimental days. In each set of experiments, taurocholate uptake into cells transfected to express sodium/taurocholate cotransporting polypeptide (NTCP) was included as a positive control for transfection and expression efficiency. Experience with this assay panel has demonstrated that inclusion of a single positive control is sufficiency, as relative activities of each transporter for reference substrates are consistent between experiments. In each set of experiments, docetaxel uptake

into the cells transfected with the vector only was included as a negative control to ensure that results were not confounded by an effect of the transfection process.

Transwell-based vectorial transport assay. Vectorial transport assays were conducted as described previously with minor modifications (24). MDCKII cells were seeded onto 12-Transwell (diameter 12 mm; pore size 0.4 μm; Corning Incorporated) at an initial density of 0.4×10^6 cells per well and grown for 3 days. Twenty-four hours before transport experiments, the cells were treated with 10 mmol/L sodium butyrate (Sigma-Aldrich) to increase protein expression. Transepithelial resistance was measured in each well using a millicell voltammeter (model ERS; Millipore); wells registering a resistance of 200 Ω or greater, after correcting for the resistance obtained in control blank wells, were used in the transport experiments (23). [^{3}H]Docetaxel was dissolved in the uptake buffer Opti-MEM 1 medium (Invitrogen) to a final concentration of 0.1 μmol/L without addition of unlabeled docetaxel. After washing cells with prewarmed uptake buffer, 0.8 mL of uptake buffer without [^{3}H]docetaxel was added to the apical compartments of the cell monolayers. The same amount (0.8 mL) of uptake buffer containing [^{3}H]docetaxel was then added to the basolateral compartments of the cell monolayers. Cells were then incubated at 37°C for given time points. After 0.5, 1, and 2 hours, aliquots (50 μL) were removed from both the apical and basolateral compartments and plates were placed back to the incubator. After 3 hours incubation, additional 50 μL were taken from both compartments and docetaxel radioactivity in media obtained at each time point was then measured by liquid scintillation counter (PerkinElmer). Finally, the cells were washed three times with ice-cold PBS buffer and were lysed with 0.2% SDS solution containing 1× protease inhibitor cocktail (Roche). Cell lysates were then used to determine the protein concentrations by the BCA Assay Kit (Thermo Fisher Scientific). To measure the activity of intracellular docetaxel, cells in Transwell were incubated for 0.5, 1, 2, and 3 hours after adding radiolabeled docetaxel (final conc. 0.1 μmol/L). The Transwell plates were taken out of the incubator at each time point. Cells were then washed, lysed, followed by measuring the radioactivity of docetaxel and determining the protein concentration as described above. All experiments were performed more than three times in > triplicates.

Docetaxel distribution in *Slco1b2*$^{-/-}$ mice

Male *Slco1b2*$^{-/-}$ mice, 21 to 24 weeks of age and male WT littermate controls, were used to determine docetaxel distribution. The radiolabeled [^{3}H]docetaxel (1 mg/kg, specific activity 30 Ci/mmol) dissolved in ethanol/0.9% saline solution was injected i.v. into the tail vein of groups of 4 mice. Blood samples from each mouse were drawn from the saphenous vein at 5 and 15 minutes after injection. After 30 minutes, mice were anesthetized with isofluorane, blood was removed by cardiac puncture and livers were harvested, weighed, and homogenized with PBS (1% w/v BSA). Total radioactivity was determined after the addition of plasma (25 μL) or liver homogenates (500 μL) to vials containing 5 mL of Ultima Gold Scintillation Cocktail (PerkinElmer LAS Canada Inc.). Docetaxel clearance after i.v. injection was calculated as dose/AUC, where AUC is the area under the plasma concentration-time profile from $t = 0$ to ∞. The protocols for the animal experiments were approved by The University of Western Ontario Animal Care Committee.

Data fitting and statistical analysis

Parameters for saturation kinetics (V_{max} and K_m) were estimated by nonlinear curve fitting using Prism (GraphPad Software, Inc.) or Scientist (Micromath Scientific Software). Determination of statistical differences between group parameters was determined using the Student *t* test, Mann–Whitney *U* test, one way ANOVA (using Tukey–Kramer multiple comparison test), or Fisher exact test, as appropriate. A *P* value of <0.05 was taken to be the minimum level of statistical significance.

Results

Docetaxel uptake is mediated by multiple OATP transporters *in vitro*

A panel of uptake transporter expression plasmids was expressed individually in HeLa cells using recombinant vaccinia and evaluated for docetaxel transport. After 10 minutes incubation, we identified several members of the human OATP family capable of docetaxel uptake, including OATP1A2, OATP1B1, OATP1B3, and OATP1C1 (Fig. 1). Rat Oatp1b2, orthologous to human OATP1B1 and OATP1B3, also showed efficient docetaxel uptake. However, not all OATPs were capable of transporting docetaxel as OATP2B1, OATP3A1, OATP4A1, and OATP5A1 demonstrated no significant docetaxel uptake. In addition, other known drug uptake transporters such as the organic anion transporters (OAT), organic cation transporters, as well as bile acid uptake transporters such as NTCP and apical sodium-dependent bile acid transporter (ASBT), exhibited no docetaxel transport.

Time course experiments indicated significant accumulation of docetaxel over control in OATP1B1-, OATP1B3-, and rat Oatp1b2-expressing HeLa cells up to 30 minutes after incubation. To gain a better understanding of the pharmacokinetic parameters of docetaxel transport mediated by hepatic OATP transporters, kinetic analysis was performed. Radiolabeled docetaxel uptake was assessed in the presence of varying concentrations of unlabeled docetaxel (0.1–50 μmol/L for OATP1B3; 0.1–300 μmol/L for OATP1B1; 0.1–100 μmol/L for Oatp1b2) for estimation of K_m

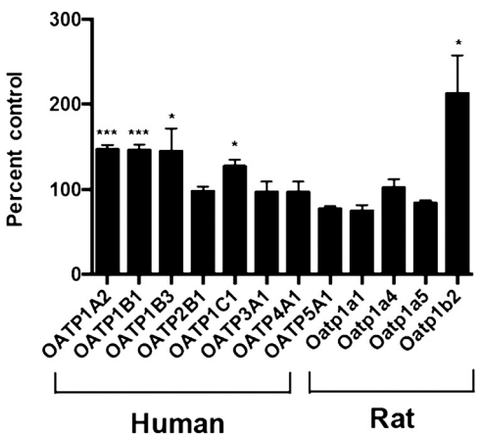

Figure 1.
Multiple OATPs transport docetaxel *in vitro*. A panel of OATP drug uptake transporters was assessed for docetaxel (0.1 μmol/L) transport activity at 10 minutes. Vector control (pEF6) was used as a reference. Multiple human OATPs, including OATP1A2, OATP1B1, OATP1B3, and OATP1C1, are capable of transporting docetaxel *in vitro*. Rat Oatp1b2 also transports docetaxel *in vitro*. Data, the percentage of cellular uptake compared with vector control (mean ± SE, $n = 6$); *, $P < 0.05$; ***, $P < 0.001$.

and V_{max}. Interestingly, kinetic analysis for OATP1B1 suggested two kinetic components for transport. An Eadie–Hofstee plot together with curve fitting indicated that, for OATP1B1, transport kinetics at concentrations up to 300 μmol/L are described by a high-affinity, low-capacity component (K_m 0.43 ± 1.32 μmol/L, V_{max} 37.7 ± 47.2 pmol/mg/min) together with a nonsaturable component that is low affinity, high capacity (Fig. 2A). Transport of docetaxel into HeLa cells transfected with OATP1B3 or Oatp1b2 was time-dependent and saturable with an K_m of 14 ± 6.5 μmol/L and 20.8 ± 7.4 μmol/L, respectively, and a maximum velocity V_{max} of 480 ± 90, and 1,548 ± 186 pmol/mg/min, respectively (Fig. 2B and C).

OATP1B1 and OATP1B3 variants differentially transport docetaxel *in vitro*.

Each panel of OATP1B1 (Supplementary Table S1) and OATP1B3 (Supplementary Table S2) nonsynonymous variants was expressed in HeLa cells and evaluated for differential transport of docetaxel *in vitro*. A number of variants were associated with significantly impaired docetaxel uptake when compared with the WT reference alleles, *SLCO1B1*1a* or *SLCO1B3*1*. Pertaining to *SLCO1B1* encoding OATP1B1, most notably, the common alleles, *SLCO1B1 521T>C* (**5*) and 388A>G/521T>C (**15*), demonstrated significantly reduced docetaxel uptake (Fig. 3A). The two reference alleles, *SLCO1B1 388G>A* (**1a*) and *SLCO1B1 388A>G* (**1b*), exhibited equivalent docetaxel transport activity. Regarding *SLCO1B3* encoding OATP1B3, several nonsynonymous SNPs were associated with impaired docetaxel transport *in vitro*, including *SLCO1B3* 699G>A, 1559A>C, 1679T>C, and 334T>G/699G>A (Fig. 3B).

Protein expression of all stable MDCKII cell lines

To investigate the directional transport activity of docetaxel, we generated MDCKII cell lines stably expressing hepatic uptake transporters OATP1B1 or OATP1B3 and/or an efflux transporter MDR1. OATP1B1, OATP1B3, and MDR1 protein expression from stable cells are shown in Fig. 4. All cell lines expressed the proteins of predicted molecular weights, whereas no significant amounts of any protein of interest were detectable in control cells (MDCKII-Co) lacking any insert. OATP1B1 in crude cell membrane fractions (Fig. 4A) showed one glycosylated form with an apparent molecular weight of 84 kDa and one unglycosylated form (58 kDa), but only glycosylated form 85 kDa was detected in cell surface proteins (Fig. 4B). These results support the previous reports that 58 kDa of OATP1B1 is an ER-attached immature form (14, 25). In this study, we did not detect constitutive OATP1B1 or OATP1B3 protein expression (Fig. 4A and B) as well as OATP1A2 in control cells by immunoblot analysis, consistent with previous reports (26–28). Furthermore, transcriptional expression of constitutive OATP1A2 and OATP1B1 had been previously noted in MDCK cells, but not in MDCKII cells (29).

Vectorial docetaxel transport is dependent on OATP1B uptake and MDR1 efflux

For vectorial transport assay, [^{3}H]docetaxel was administered to the basal compartment of cell monolayers of control (MDCKII-Co), single (MDCKII-OATP1B1, MDCKII-OATP1B3, and MDCKII-MDR1)-, and double (MDCKII-OATP1B1/MDR1 and MDCKII-OATP1B3/MDR1)-transfected cells. There was no

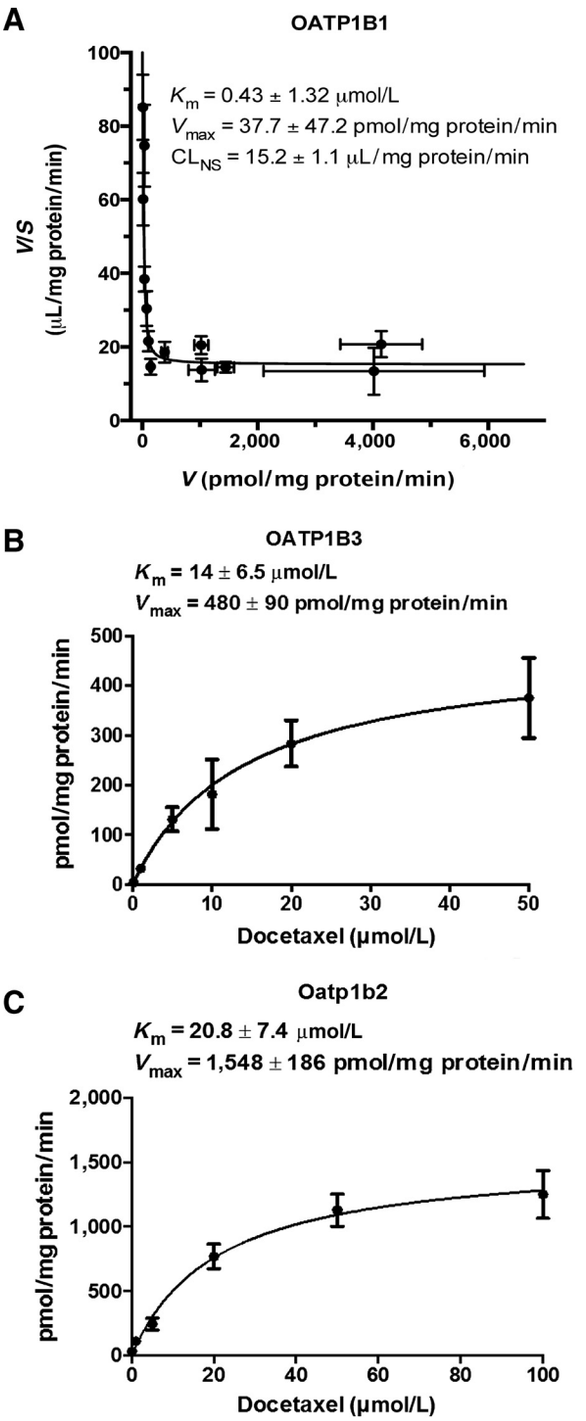

Figure 2.
Docetaxel transport kinetics. An Eadie–Hofstee plot at a broad range of concentrations (0.1–300 μmol/L; A) for OATP1B1 showed a high-affinity, low-capacity component (K_m 0.43 ± 1.32 μmol/L, V_{max} 37.7 ± 47.2 pmol/mg/min) together with a nonsaturable component that is low-affinity, high-capacity (V, reaction rate; S, substrate concentration). Michaelis–Menten-type nonlinear curve fittings are demonstrated for OATP1B3 (0.1–50 μmol/L; B) and Oatp1b2 (0.1–100 μmol/L; C). Data, mean ± SE (n = 8 for OATP1B3 and Oatp1b2;n = 12 for OATP1B1).

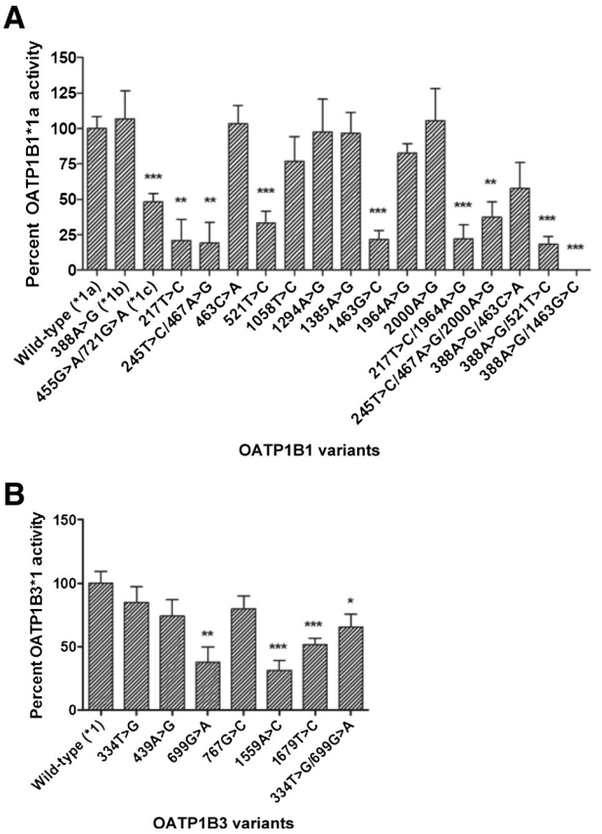

Figure 3.
OATP1B1 and OATP1B3 variants differentially transport docetaxel *in vitro*. Uptake of radiolabeled docetaxel (0.1 μmol/L) at 20 minutes by HeLa cells transfected with OATP1B1 or OATP1B3 variants was assessed relative to WT *OATP1B1*1a* and *OATP1B3*1*, respectively. The commonly occurring *SLCO1B1* variants *521T>C (*5)* and *388A>G/521T>C (*15)* were associated with significantly impaired docetaxel transport. There was no significant differences in transport between the two reference alleles *SLCO1B1 388G>A* (**1a*) and *SLCO1B1 388A>G* (**1b*; A). Several *SLCO1B3* variants, including *699G>A*, *1559A>C*, *1679T>C*, and *334T>G/699G>A*, were associated with impaired docetaxel transport (B). Values are expressed as the percentage of cellular uptake by *OATP1B1*1a* or *OATP1B3*1* (mean ± SE, $n = 6$); *, $P < 0.05$; **, $P < 0.01$; ***, $P < 0.001$.

significant difference between MDCKII-Co and MDCKII-OATP1B1 or MDCKII-OATP1B3 cells at incubation of 0.5 hours, but after 0.5 hours the apical docetaxel accumulation in MDCKII-OATP1B1 and MDCKII-OATP1B3 cells was significantly higher compared with MDCKII-Co cells (Fig. 5A and B). In contrast, at 0.5 hours, docetaxel transported into the apical compartment of double-transfected MDCKII-OATP1B1/MDR1 and MDCKII-OATP1B3/MDR1 cells was significantly higher than in single-transfected MDCKII-OATP1B1 and MDCKII-OATP1B3 cells, respectively ($P < 0.001$ for OATP1B1; $P < 0.01$ for OATP1B3). This pattern continued up to 3 hours. Interestingly, the apical docetaxel was significantly higher in MDCKII-MDR1 cells expressing MDR1 only than in MDCKII-Co cells over time ($P < 0.05$).

To examine intracellular docetaxel, [^{3}H]docetaxel was administrated to the basal compartment of cell monolayers in Transwell and cells were incubated for 0.5, 1, 2, and 3 hours. The Transwell plates were taken out of the incubator at each time point and cells were then analyzed for intracellular accumulation of docetaxel. As shown in Fig. 5C and D, intracellular accumulation of docetaxel was significantly increased in MDCKII-OATP1B1 and MDCKII-OATP1B3 cells over MDCKII-Co cells at 0.5 and 1 hours time points, but uptake appeared to be saturable at later time points, reflecting efficient active uptake at early time points. Intracellular docetaxel was significantly lower in the double-transfected MDCKII-OATP1B1/MDR1 ($P < 0.001$) and MDCKII-OATP1B3/MDR1 cells ($P < 0.01$) compared with the single-transfected MDCKII-OATP1B1 and MDCKII-OATP1B3 cells at all time points, respectively. Accordingly, considerably higher amounts of docetaxel were found in the apical compartment of double-transfected MDCKII-OATP1B1/MDR1 and MDCKII-OATP1B3/MDR1 cells compared with single-transfected MDCKII-OATP1B1 and MDCKII-OATP1B3 cells (Fig. 5A and B). Vectorial transport studies were also conducted up to 4 hours incubation time. In this experiment, cellular translocation of docetaxel was markedly greater when [^{3}H]docetaxel was administrated to the basal side of all cultured cells, including single- and double-transfected cells, and its presence measured on the apical side (basal-to-apical) compared with addition of docetaxel to the opposite compartment (apical-to-basal). Moreover, the amount of docetaxel transported into the basal side (apical-to-basal) was maintained at baseline over time.

Slco1b2$^{-/-}$ mice significantly alter docetaxel disposition

We performed experiments in *Slco1b2*$^{-/-}$ mice to assess the role of hepatic OATP1B to the *in vivo* disposition of docetaxel. As the initial article describing *Slco1b2*$^{-/-}$ mice demonstrated modest gender-dependent differences in *Slco1a4* and *Slco2b1* expression in female *Slco1b2*$^{-/-}$ mice only (30), we used male *Slco1b2*$^{-/-}$ mice for docetaxel transport experiments to eliminate any confounding by compensatory effects in other Oatp transporters. Male *Slco1b2*$^{-/-}$ mice (ages 21–24 weeks) and male WT littermate controls were used for docetaxel distribution experiments. As shown in Fig. 6A, there were significantly higher plasma docetaxel levels in mice lacking Oatp1b2 expression at given time points assessed. The plasma AUC in *Slco1b2*$^{-/-}$ mice was approximately 5.5-fold greater than in WT mice (mean docetaxel plasma AUC ± SD: WT, 340 ± 149 ng·h/mL; *Slco1b2*$^{-/-}$, 62 ± 8 ng·h/mL, $P < 0.05$). Although there was no significant difference in docetaxel liver concentrations in *Slco1b2*$^{-/-}$ mice compared with WT mice (data not shown), the liver-to-plasma ratio was approximately 3-fold decreased (Fig. 6B) in *Slco1b2*$^{-/-}$ mice ($P < 0.05$). The plasma clearance of docetaxel in *Slco1b2*$^{-/-}$ mice was 83% lower than WT mice (mean plasma clearance ± SD: WT mice, 473 ± 124 mL/h/kg; *Slco1b2*$^{-/-}$ mice, 73 ± 35 mL/h/kg; $P < 0.05$).

Discussion

In this study, we conducted a systematic evaluation to define relevant OATP transporters responsible for docetaxel uptake and clearance. We identified multiple OATPs, including human OATP1A2, OATP1B1, OATP1B3, and OATP1C1, capable of transporting docetaxel *in vitro*. Rat Oatp1b2 was also capable of docetaxel transport *in vitro* and *in vivo*. As OATP1B1 and OATP1B3 are expressed primarily at the basolateral membrane of hepatocytes (17), this would suggest potential important roles for these transporters in the hepatic uptake of docetaxel. Kinetic analysis of docetaxel transport revealed similar kinetic parameters among OATP1B/1b transporters. In addition, a MDCKII stable cell system revealed an effective transcellular transport activity of docetaxel

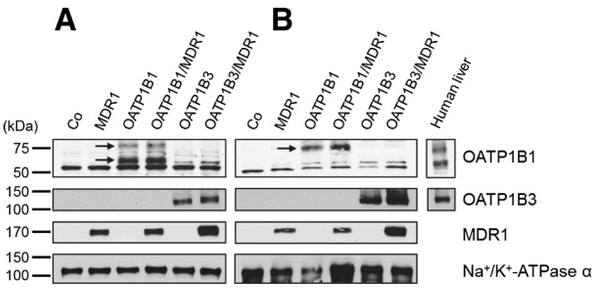

Figure 4.
Immunoblot analyses of OATP1B1, OATP1B3, and MDR1 expressions in MDCKII-control cells (Co), single (OATP1B1, OATP1B3, and MDR1) and double (OATP1B1/MDR1 and OATP1B3/MDR1) cell lines. Crude cell membrane fractions (A) and biotinylated cell surface proteins (B) were subjected to 10% SDS polyacrylamide gels, and then transferred onto nitrocellulose membranes. The blots were probed or reprobed with different antibodies, including OATP1B1, OATP1B3, MDR1, and Na^+/K^+-ATPase α antibodies. Whereas OATP1B1 in crude cell membrane fractions showed one glycosylated form 84 kDa and one unglycosylated form 58 kDa, only a glycosylated form 85 kDa of OATP1B1 was detected in cell surface proteins (arrows). OATP1B3 showed one band with approximately 120 kDa and MDR1 one with 170 kDa. Human liver extracts were used as a positive control.

mediated by recombinant human OATP1B and MDR1 transporters in double-transfected cells.

Contrary to our findings, previous studies demonstrated that docetaxel is a substrate for OATP1B3, not OATP1B1, in studies of the Xenopus laevis oocyte transporter expression system (3, 18). The reason underlying the discrepancies is unclear, but may be related to intrinsic differences in expression systems or time points at which uptake was determined. In addition, we previously indicated differential hepatic expression patterns for OATP1B1 and OATP1B3: In immunohistochemical analysis using normal human liver sections, OATP1B1 exhibited a diffuse staining pattern throughout liver sections whereas OATP1B3 showed a more restricted staining pattern with the greatest degree of expression being confined to perivenous distribution (14). Although OATP1B1 and OATP1B3 are important determinants of hepatic uptake of drug substrates, it is unclear whether the differences in hepatic expression have significant clinical implications for drug disposition. Congruent with our results, a recent study reported by de Graan and colleagues (5) indicated that docetaxel uptake was facilitated by OATP1B1 and OATP1B3 in HEK293 or CHO cells expressing these transporters whereas only OATP1B3 constructs in Xenopus laevis oocytes, but not OATP1B1, exhibited docetaxel transport, illustrating that differences in expression systems may account for discrepancies in docetaxel substrate specificity.

Mice deficient in Oatp transporters have been generated and functionally characterized for *in vivo* transport of endogenous or xenobiotic OATP substrates (30, 31). Mouse Oatp1b2 is orthologous to human OATP1B1 and OATP1B3 (32). *Slco1b2*$^{-/-}$ mice are fertile, develop normally, and have no overt phenotypic abnormalities (30). However, these mice significantly altered the hepatic disposition of the prototypical OATP drug substrates

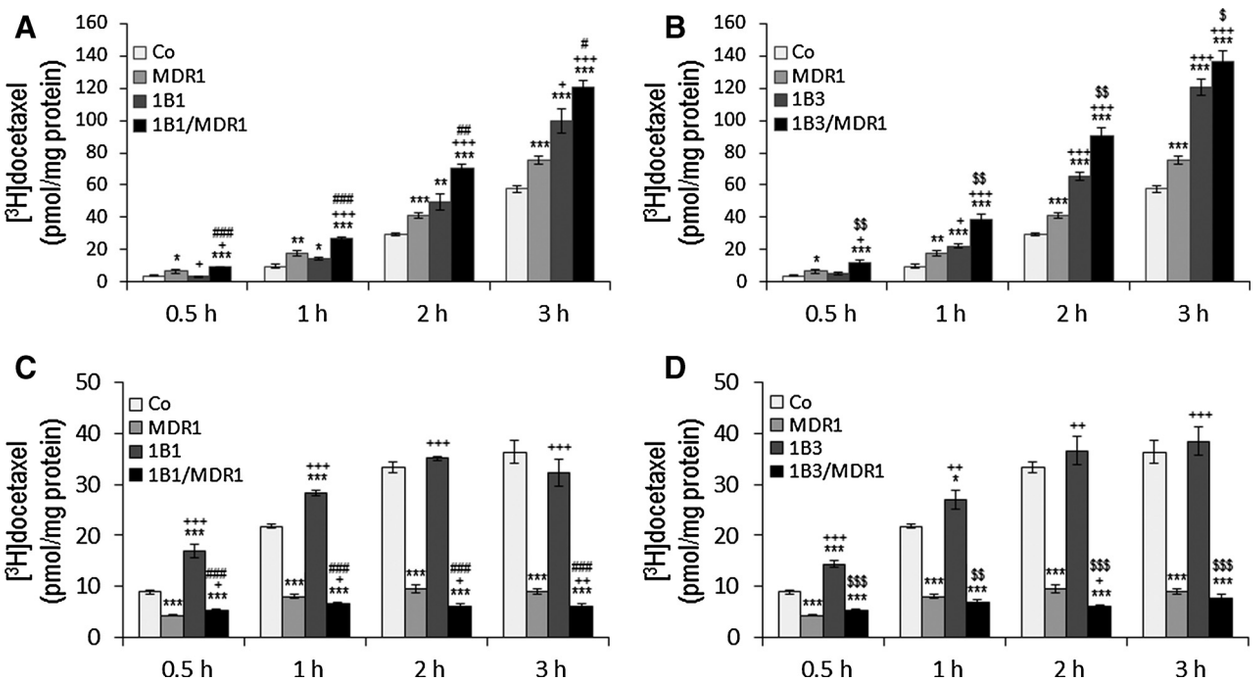

Figure 5.
Vectorial transport and intracellular accumulation of radiolabeled docetaxel. [^{3}H]Docetaxel (0.1 μmol/L) was administered to the basal compartment of monolayers of MDCKII-control (Co), single (MDR1, OATP1B1, and OATP1B3) and double (OATP1B1/MDR1 and OATP1B3/MDR1) cell lines. After 0.5, 1, 2, and 3 hours of incubation, translocation of docetaxel into the apical compartment (A and B) and intracellular accumulation of docetaxel (C and D) are shown. Whereas apical docetaxel was significantly higher in MDCKII-OATP1B1/MDR1 and MDCKII-OATP1B3/MDR1 cells compared with MDCKII-OATP1B1 and MDCKII-OATP1B3 cells, respectively, at all time points, intracellular docetaxel was significantly lower in MDCKII-OATP1B1/MDR1 and MDCKII-OATP1B3/MDR1 cells. Data, mean ± SE ($n = 6$ for vectorial transport study; $n = 4$ for intracellular accumulation study); *, $P < 0.05$; **, $P < 0.01$; and ***, $P < 0.001$ versus MDCKII-Co cells; $^{+}$, $P < 0.05$; $^{++}$, $P < 0.01$; and $^{+++}$, $P < 0.001$ versus MDCKII-MDR1 cells; $^{\#}$, $P < 0.05$; $^{\#\#}$, $P < 0.01$; and $^{\#\#\#}$, $P < 0.001$ versus MDCKII-OATP1B1 cells; $^{\$}$, $P < 0.05$; $^{\$\$}$, $P < 0.01$; and $^{\$\$\$}$, $P < 0.001$ versus MDCKII-OATP1B3 cells.

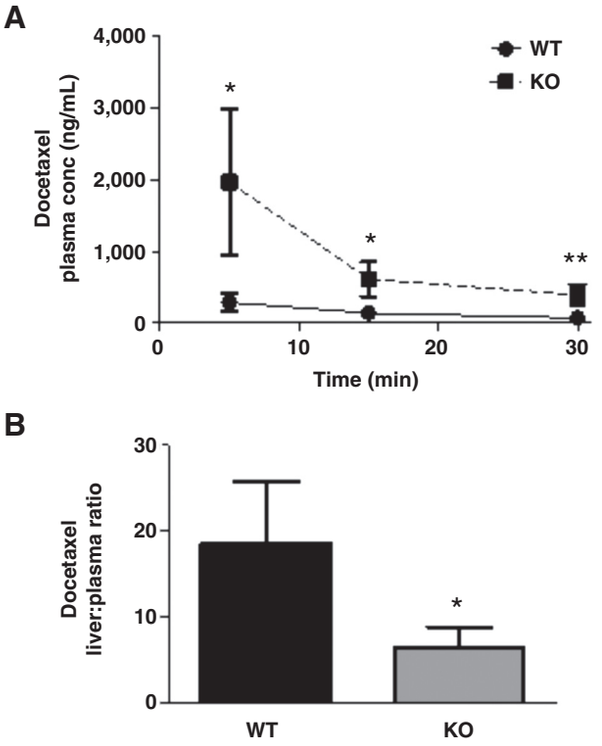

Figure 6.
Docetaxel disposition studies in *Slco1b2*$^{-/-}$ mice. *Slco1b2*$^{-/-}$ knockout mice (KO) have significantly higher docetaxel plasma AUC than WT mice (A). Measured after a single i.v. dose 1 mg/kg [^{3}H]docetaxel (30 Ci/mmol). Blood was sampled from the saphenous vein of each mouse at 5, 15, and 30 minutes after injection. *Slco1b2*$^{-/-}$ mice have a significantly lower docetaxel liver: plasma ratio compared with WT mice (B). Data, mean ± SD; *, $P < 0.05$; **, $P < 0.01$; ($n = 4$/group; 21–24 weeks).

pravastatin and rifampin *in vivo* (30). Another Oatp mouse model, *Slco1a/1b*$^{-/-}$ mice, significantly decreased the hepatic uptake of drug substrates such as methotrexate and fexofenadine (31). These studies illustrate the important roles of these animal models for understanding the *in vivo* roles of hepatic OATP transporters in drug disposition.

Accordingly, we further extended the findings from our *in vitro* experiments in *Slco1b2*$^{-/-}$ mice to assess the role of hepatic OATPs to the *in vivo* disposition of docetaxel. The plasma AUC in *Slco1b2*$^{-/-}$ mice was approximately 5.5-fold greater than in WT mice whereas the liver-to-plasma ratio was approximately 3-fold decreased in *Slco1b2*$^{-/-}$ mice. Importantly, the plasma clearance of docetaxel in *Slco1b2*$^{-/-}$ mice was 83% lower than WT mice. Although a previous study demonstrated a dramatically increased docetaxel AUC and 18-fold decreased clearance in *Slco1b2*$^{-/-}$ mice (5), follow-up studies from this group have confirmed that the contribution of Oatp1b transporters to docetaxel disposition is more in line with results from our study (33). Moreover, it is known that docetaxel is a substrate of the efflux transporter MDR1 (P-gp; ref. 34). However, studies conducted in P-gp knockout mice (*Mdr1a/1b*$^{-/-}$) indicated that the AUC of docetaxel following i.v. administration was similar in knockout and WT mice, suggesting that mechanisms other than efflux contribute significantly to hepatic clearance of docetaxel (35). Finally, our vectorial transport assay *in vitro* showed a higher docetaxel transport in the apical compartment of the cell monolayers of the double-transfected OATP1B and MDR1 cells compared with the single-transfected MDR1 cells. Collectively, our studies suggest that hepatic OATP1B transporters are critical to the hepatic clearance of docetaxel, strongly supporting that the liver as a major organ for docetaxel distribution and hepatic OATPs plays significant roles in docetaxel disposition.

The various processes mediating drug elimination, either through metabolic breakdown or excretion, can substantially affect interindividual variability in drug handling. Polymorphisms in CYP3A4 and MDR1 have been identified and characterized (36, 37). Several studies found no significant differences between *ABCB1* genotype and docetaxel clearance in Asian or Caucasian cancer patients (3, 38). Another study assessed variants in CYP3A4/5 for associations with docetaxel pharmacokinetics (3). The combination of the *CYP3A4*1B* and *CYP3A5*1A* alleles (*CYP3A4/5*2* haplotype) was associated with a 64% increase in docetaxel clearance independent of sex and CYP3A activity, but this haplotype was only noted in 6 of 92 patients and likely only explains a very minor proportion of interindividual variability in docetaxel pharmacokinetics.

There has been significant effort in studying polymorphisms in *SLCO* genes as potential determinants of interindividual variability in drug disposition. To date, the functional consequences of polymorphism in the hepatic uptake transporter OATP1B1 have received the most attention. A common SNP, 521T>C (Val174Ala; *SLCO1B1*5*), has frequencies of approximately 15%, 2%, and 15% in Caucasians, African-Americans, and Asians, respectively (21, 39). The apparent mechanisms for impaired function for many functionally relevant OATP1B1 variants, including the 521T>C variant, are due to either decreased protein expression or impaired trafficking of the protein to the membrane (21). The pharmacokinetics of a growing number of drugs appear to be dependent on *SLCO1B1* 521T>C genotype, including pitavastatin, rosuvastatin, fexofenadine, ezetimibe, and nateglinide (40–44). Notably, this allele was associated with a significant increased risk for simvastatin-induced myopathy in a genomewide association study (45). More recently, functionally relevant nonsynonymous polymorphisms have also been identified in *SLCO1B3* and associated with impaired *in vitro* transport of substrates such as cholecystokinin (CCK8) and rosuvastatin (22). Two variants, 1559A>C and 1679T>C, were associated with significantly reduced total and cell surface protein expression. However, the clinical relevance of genetic heterogeneity in *SLCO1B3* to drug disposition is unclear at this time.

We explored the potential roles of *SLCO1B1* and *SLCO1B3* SNPs to docetaxel disposition. Either of two reference alleles, A388 (*OATP1B1*1a*) or G388 (*OATP1B1*1b*), demonstrated equivalent transport activity. A number of *SLCO1B1* SNPs were associated with impaired docetaxel transport *in vitro*. In particular, the commonly occurring 521T>C (**5*) variant as well as the **15 variant (**1b+*5*), were both associated with significantly impaired docetaxel transport activity. Furthermore, several *SCLO1B3* variants, including 1559A>C and 1679T>C, were also associated with significantly impaired docetaxel transport. Interestingly, as docetaxel has been demonstrated to be an OATP1B3 substrate, *SLCO1B3* SNPs have also been evaluated in relation to docetaxel disposition and response. Baker and colleagues (3) found no signification association between six nonsynonymous SNPs in *SLCO1B3* and docetaxel clearance in a population of Caucasian adult oncology patients. In contrast, Kiyotani and

colleagues (46) identified a noncoding intronic SNP in *SLCO1B3* (rs11045585) that was associated with a significantly higher risk for docetaxel-induced leucopenia/neutropenia in a population of Japanese adult oncology patients. Finally, de Graan and colleagues (5) found no significant differences in docetaxel clearance among a predominantly white adult oncology population ($n = 141$) when assessed for commonly occurring polymorphisms in *SLCO1B1* or *1B3*. As OATP1B1 and OATP1B3 are both expressed at the basolateral membrane of hepatocytes and can facilitate docetaxel uptake, it is possible that a potential loss of docetaxel uptake associated with polymorphic variant in either OATP1B1 or 1B3 may be compensated for by the other OATP1B transporter, thereby mitigating the influence of the polymorphism on hepatic clearance. However, additional clinical PK:PG correlative studies in larger populations of patients may clarify the relevance of OATP1B polymorphisms to the wide variability in docetaxel pharmacokinetics.

In conclusion, we describe important roles for hepatic OATPs, including OATP1B1 and OATP1B3, to the disposition of docetaxel. Through a series of *in vitro* and *in vivo* experiments, we demonstrate that hepatic OATP1B transporters play significant roles in the hepatic uptake, clearance, and plasma exposure of docetaxel. Moreover, we indicate that commonly occurring *SLCO1B1* and *SLCO1B3* variants differentially transport docetaxel *in vitro*, which may contribute to the oft-witnessed wide interindividual variability in docetaxel disposition and response. Accordingly, our findings reveal important insights into the relevance of hepatic OATPs to the clinical pharmacology of docetaxel. In addition, we suggest that docetaxel is transported by multiple OATPs, which may also play important roles on docetaxel disposition, pharmacokinetics, and toxicities.

Disclosure of Potential Conflicts of Interest

No potential conflicts of interest were disclosed.

Authors' Contributions

Conception and design: H.H. Lee, W. Teft, R.G. Tirona, R.B. Kim, R.H. Ho
Development of methodology: H.H. Lee, R.H. Ho
Acquisition of data (provided animals, acquired and managed patients, provided facilities, etc.): B.F. Leake, W. Teft, R.H. Ho
Analysis and interpretation of data (e.g., statistical analysis, biostatistics, computational analysis): H.H. Lee, W. Teft, R.G. Tirona, R.B. Kim, R.H. Ho
Writing, review, and/or revision of the manuscript: H.H. Lee, R.G. Tirona, R.B. Kim, R.H. Ho
Administrative, technical, or material support (i.e., reporting or organizing data, constructing databases): B.F. Leake
Study supervision: R.B. Kim, R.H. Ho
Other (conducted experiments): H.H. Lee

Grant Support

This project was supported by grants from Hyundai Hope on Wheels (to R.H. Ho), NIH R01 GM099924 (to R.H. Ho), and Canadian Institutes of Health Research (CIHR) grants (MOP-8975 and DSEN-PREVENT FRN-117588; to R.B. Kim).

The costs of publication of this article were defrayed in part by the payment of page charges. This article must therefore be hereby marked advertisement in accordance with 18 U.S.C. Section 1734 solely to indicate this fact.

Received June 26, 2014; revised January 21, 2015; accepted February 10, 2015; published OnlineFirst February 18, 2015.

References

1. Baker SD, Sparreboom A, Verweij J. Clinical pharmacokinetics of docetaxel: recent developments. Clin Pharmacokinet 2006;45:235–52.
2. Bruno R, Hille D, Riva A, Vivier N, ten Bokkel Huinnink WW, van Oosterom AT, et al. Population pharmacokinetics/pharmacodynamics of docetaxel in phase II studies in patients with cancer. J Clin Oncol 1998;16:187–96.
3. Baker SD, Verweij J, Cusatis GA, vanSchaik RH, Marsh S, Orwick SJ, et al. Pharmacogenetic pathway analysis of docetaxel elimination. Clin Pharmacol Ther 2009;85:155–63.
4. Jabir RS, Naidu R, Annuar MA, Ho GF, Munisamy M, Stanslas J. Pharmacogenetics of taxanes: impact of gene polymorphisms of drug transporters on pharmacokinetics and toxicity. Pharmacogenomics 2012;13:1979–88.
5. de Graan AJ, Lancaster CS, Obaidat A, Hagenbuch B, Elens L, Friberg LE, et al. Influence of polymorphic OATP1B-type carriers on the disposition of docetaxel. Clin Cancer Res 2012;18:4433–40.
6. Kim KP, Ahn JH, Kim SB, Jung KH, Yoon DH, Lee JS, et al. Prospective evaluation of the drug-metabolizing enzyme polymorphisms and toxicity profile of docetaxel in Korean patients with operable lymph node-positive breast cancer receiving adjuvant chemotherapy. Cancer Chemother Pharmacol 2012;69:1221–7.
7. Tsai SM, Lin CY, Wu SH, Hou LA, Ma H, Tsai LY, et al. Side effects after docetaxel treatment in Taiwanese breast cancer patients with CYP3A4, CYP3A5, and ABCB1 gene polymorphisms. Clin Chim Acta 2009;404:160–5.
8. Tran A, Jullien V, Alexandre J, Rey E, Rabillon F, Girre V, et al. Pharmacokinetics and toxicity of docetaxel: role of CYP3A, MDR1, and GST polymorphisms. Clin Pharmacol Ther 2006;79:570–80.
9. van Herwaarden AE, Wagenaar E, van der Kruijssen CM, van Waterschoot RA, Smit JW, Song JY, et al. Knockout of cytochrome P450 3A yields new mouse models for understanding xenobiotic metabolism. J Clin Invest 2007;117:3583–92.
10. Wils P, Phung-Ba V, Warnery A, Lechardeur D, Raeissi S, Hidalgo IJ, et al. Polarized transport of docetaxel and vinblastine mediated by P-glycoprotein in human intestinal epithelial cell monolayers. Biochem Pharmacol 1994;48:1528–30.
11. Gottesman MM, Pastan I. Biochemistry of multidrug resistance mediated by the multidrug transporter. Annu Rev Biochem 1993;62:385–427.
12. Leveque D, Jehl F. P-glycoprotein and pharmacokinetics. Anticancer Res 1995;15:331–6.
13. Cortes JE, Pazdur R. Docetaxel. J Clin Oncol 1995;13:2643–55.
14. Ho RH, Tirona RG, Leake BF, Glaeser H, Lee W, Lemke CJ, et al. Drug and bile acid transporters in rosuvastatin hepatic uptake: function, expression, and pharmacogenetics. Gastroenterology 2006;130:1793–806.
15. Hagenbuch B, Meier PJ. The superfamily of organic anion transporting polypeptides. Biochim Biophys Acta 2003;1609:1–18.
16. Iusuf D, van de Steeg E, Schinkel AH. Functions of OATP1A and 1B transporters *in vivo*: insights from mouse models. Trends Pharmacol Sci 2012;33:100–8.
17. Hagenbuch B, Gui C. Xenobiotic transporters of the human organic anion transporting polypeptides (OATP) family. Xenobiotica 2008;38:778–801.
18. Smith NF, Acharya MR, Desai N, Figg WD, Sparreboom A. Identification of OATP1B3 as a high-affinity hepatocellular transporter of paclitaxel. Cancer Biol Ther 2005;4:815–8.
19. Ho RH, Leake BF, Roberts RL, Lee W, Kim RB. Ethnicity-dependent polymorphism in Na+taurocholate cotransporting polypeptide (SLC10A1) reveals a domain critical for bile acid substrate recognition. J Biol Chem 2004;279:7213–22.
20. Blakely RD, Clark JA, Rudnick G, Amara SG. Vaccinia-T7 RNA polymerase expression system: evaluation for the expression cloning of plasma membrane transporters. Anal Biochem 1991;194:302–8.
21. Tirona RG, Leake BF, Merino G, Kim RB. Polymorphisms in OATP-C: identification of multiple allelic variants associated with altered transport activity among European- and African-Americans. J Biol Chem 2001;276:35669–75.
22. Schwarz UI, Meyer zu Schwabedissen HE, Tirona RG, Suzuki A, Leake BF, Mokrab Y, et al. Identification of novel functional organic anion-

transporting polypeptide 1B3 polymorphisms and assessment of substrate specificity. Pharmacogenetics Genomics 2011;21:103–14.
23. Kim RB, Fromm MF, Wandel C, Leake B, Wood AJ, Roden DM, et al. The drug transporter P-glycoprotein limits oral absorption and brain entry of HIV-1 protease inhibitors. J Clin Invest 1998;101:289–94.
24. Fahrmayr C, Konig J, Auge D, Mieth M, Munch K, Segrestaa J, et al. Phase I and II metabolism and MRP2-mediated export of bosentan in a MDCKII-OATP1B1-CYP3A4-UGT1A1-MRP2 quadruple-transfected cell line. Br J Pharmacol 2013;169:21–33.
25. Konig J, Cui Y, Nies AT, Keppler D. Localization and genomic organization of a new hepatocellular organic anion transporting polypeptide. J Biol Chem 2000;275:23161–8.
26. Kopplow K, Letschert K, Konig J, Walter B, Keppler D. Human hepatobiliary transport of organic anions analyzed by quadruple-transfected cells. Mol Pharmacol 2005;68:1031–8.
27. Sasaki M, Suzuki H, Ito K, Abe T, Sugiyama Y. Transcellular transport of organic anions across a double-transfected Madin-Darby canine kidney II cell monolayer expressing both human organic anion-transporting polypeptide (OATP2/SLC21A6) and Multidrug resistance-associated protein 2 (MRP2/ABCC2). J Biol Chem 2002;277:6497–503.
28. Konig J, Cui Y, Nies AT, Keppler D. A novel human organic anion transporting polypeptide localized to the basolateral hepatocyte membrane. Am J Physiol Gastrointest Liver Physiol 2000;278:G156–64.
29. Goh LB, Spears KJ, Yao D, Ayrton A, Morgan P, Roland Wolf C, et al. Endogenous drug transporters in *in vitro* and *in vivo* models for the prediction of drug disposition in man. Biochem Pharmacol 2002;64:1569–78.
30. Zaher H, Meyer zu Schwabedissen HE, Tirona RG, Cox ML, Obert LA, Agrawal N, et al. Targeted disruption of murine organic anion-transporting polypeptide 1b2 (Oatp1b2/Slco1b2) significantly alters disposition of prototypical drug substrates pravastatin and rifampin. Mol Pharmacol 2008;74:320–9.
31. van de Steeg E, Wagenaar E, van der Kruijssen CM, Burggraaff JE, de Waart DR, Elferink RP, et al. Organic anion transporting polypeptide 1a/1b-knockout mice provide insights into hepatic handling of bilirubin, bile acids, and drugs. J Clin Invest 2010;120:2942–52.
32. Fischer WJ, Altheimer S, Cattori V, Meier PJ, Dietrich DR, Hagenbuch B. Organic anion transporting polypeptides expressed in liver and brain mediate uptake of microcystin. Toxicol Appl Pharmacol 2005;203:257–63.
33. Sparreboom A, Mathijssen RH. Hepatic uptake transporters and docetaxel disposition in mice-letter. Clin Cancer Res 2014;20:4167.
34. Bardelmeijer HA, Ouwehand M, Buckle T, Huisman MT, Schellens JH, Beijnen JH, et al. Low systemic exposure of oral docetaxel in mice resulting from extensive first-pass metabolism is boosted by ritonavir. Cancer Res 2002;62:6158–64.
35. van Waterschoot RA, Lagas JS, Wagenaar E, Rosing H, Beijnen JH, Schinkel AH. Individual and combined roles of CYP3A, P-glycoprotein (MDR1/ABCB1) and MRP2 (ABCC2) in the pharmacokinetics of docetaxel. Int J Cancer 2010;127:2959–64.
36. Zhou SF, Di YM, Chan E, Du YM, Chow VD, Xue CC, et al. Clinical pharmacogenetics and potential application in personalized medicine. Curr Drug Metab 2008;9:738–84.
37. Chinn LW, Kroetz DL. ABCB1 pharmacogenetics: progress, pitfalls, and promise. Clin Pharmacol Ther 2007;81:265–9.
38. Cox MC, Low J, Lee J, Walshe J, Denduluri N, Berman A, et al. Influence of garlic (Allium sativum) on the pharmacokinetics of docetaxel. Clin Cancer Res 2006;12:4636–40.
39. Ho RH, Choi L, Lee W, Mayo G, Schwarz UI, Tirona RG, et al. Effect of drug transporter genotypes on pravastatin disposition in European- and African-American participants. Pharmacogenet Genomics 2007;17:647–56.
40. Chung JY, Cho JY, Yu KS, Kim JR, Oh DS, Jung HR, et al. Effect of OATP1B1 (SLCO1B1) variant alleles on the pharmacokinetics of pitavastatin in healthy volunteers. Clin Pharmacol Ther 2005;78:342–50.
41. Lee E, Ryan S, Birmingham B, Zalikowski J, March R, Ambrose H, et al. Rosuvastatin pharmacokinetics and pharmacogenetics in white and Asian subjects residing in the same environment. Clin Pharmacol Ther 2005;78:330–41.
42. Niemi M, Backman JT, Kajosaari LI, Leathart JB, Neuvonen M, Daly AK, et al. Polymorphic organic anion transporting polypeptide 1B1 is a major determinant of repaglinide pharmacokinetics. Clin Pharmacol Ther 2005;77:468–78.
43. Oswald S, Giessmann T, Luetjohann D, Wegner D, Rosskopf D, Weitschies W, et al. Disposition and sterol-lowering effect of ezetimibe are influenced by single-dose coadministration of rifampin, an inhibitor of multidrug transport proteins. Clin Pharmacol Ther 2006;80:477–85.
44. Zhang W, He YJ, Han CT, Liu ZQ, Li Q, Fan L, et al. Effect of SLCO1B1 genetic polymorphism on the pharmacokinetics of nateglinide. Br J Clin Pharmacol 2006;62:567–72.
45. Link E, Parish S, Armitage J, Bowman L, Heath S, Matsuda F, et al. SLCO1B1 variants and statin-induced myopathy—a genomewide study. N Engl J Med 2008;359:789–99.
46. Kiyotani K, Mushiroda T, Kubo M, Zembutsu H, Sugiyama Y, Nakamura Y. Association of genetic polymorphisms in SLCO1B3 and ABCC2 with docetaxel-induced leukopenia. Cancer Sci 2008;99:967–72.